horticulturae

MDPI

Article

Identification and Functional Analysis of the Flower Development-Related *TCP* Genes in *Erycina pusilla*

Yu-Huan Tang, Ying-Yin Zhong and Xia Huang *

Guangdong Provincial Key Laboratory of Plant Resources, School of Life Sciences, Sun Yat-sen University, Guangzhou 510275, China; touroyuu@gmail.com (Y.-H.T.); zhongyy65@mail2.sysu.edu.cn (Y.-Y.Z.)
* Correspondence: huangxia@mail.sysu.edu.cn

Abstract: Orchid flowers have evolved in concert with pollinators to form highly specialized structures resulting in zygomorphy. In dicotyledons, it is widely accepted that *CYC*-like genes are involved in the dorsoventral polarity establishment of flowers, which determines the development of zygomorphic flowers. However, the function of TCP transcription factors involved in orchid floral development is rarely known. Here, we found 15 unigenes with TCP domain (*EpTCPs*) from the previously reported *Erycina pusilla* unigene database. The expression patterns of *EpTCPs* in various tissues and different floral organs were successively detected by quantitative real-time PCR. The results revealed that the *CYC*-like gene (*EpTCP25*) and *CIN*-like genes (*EpTCP11* and *EpTCP26*) were highly expressed in inflorescences but lowly expressed in leaves and roots. What is more, these three genes were expressed relatively high in the dorsal labellum, and *EpTCP26* showed differential expression along the dorsoventral polarity of tepals, which was high in the dorsal and low in the ventral. Ectopic expression of *EpTCP25* in *Arabidopsis* repressed primary root growth and delayed flowering. *EpTCP26* overexpression in *Arabidopsis* promoted primary root growth and leaf growth. In contrast, *EpTCP11* overexpression repressed primary root growth and changed the radially symmetric flower to a bilaterally symmetric flower by inhibiting the elongation of one or two adjacent petals. In addition, the homeotic transition of floral organs is generated when these genes are ectopically expressed in *Arabidopsis*, suggesting their roles in floral morphogenesis. Altogether, our results indicate that *CIN*-like genes would be associated with the unique flower pattern development of *Erycina pusilla*.

Keywords: *Erycina pusilla*; TCP transcription factor; expression pattern; function analysis

check for updates

Citation: Tang, Y.-H.; Zhong, Y.-Y.; Huang, X. Identification and Functional Analysis of the Flower Development-Related *TCP* Genes in *Erycina pusilla*. *Horticulturae* **2024**, *10*, 534. https://doi.org/10.3390/horticulturae10060534

Academic Editor: Genhua Niu

Received: 3 April 2024
Revised: 11 May 2024
Accepted: 17 May 2024
Published: 21 May 2024

Copyright: © 2024 by the authors. Licensee MDPI, Basel, Switzerland. This article is an open access article distributed under the terms and conditions of the Creative Commons Attribution (CC BY) license (https://creativecommons.org/licenses/by/4.0/).

1. Introduction

Orchidaceae is one of the largest and most evolutionary families in the plant kingdom [1]. The flower of the orchid has evolved in concert with insects to form highly specialized structures, so the orchid is considered to be one of the ideal plants for the study of floral developmental biology in monocotyledons. The typical orchid flower is bilaterally symmetrical and includes three whorls of floral organs: the outer whorl consists of three outer tepals (named sepals); the second whorl consists of two ventral inner tepals (named petals) and a highly specified dorsal inner tepal (named labellum); and the third whorl is a column, which is the reproductive structure consisting of fused male stamen and female tissues.

Previous research on the genetic mechanism of orchid zygomorphy flower development mainly focuses on exploring how the orthologous MADS-box genes involved in the ABCDE model participate in the development and evolution of highly specialized floral organs in orchids [2–9]. The 'Orchid Code' and 'Perianth Code' models are used to demonstrate that AP3-like and AGL6-like MADS-box transcription factors play essential roles in different floral organ formations [8,10,11]. In *Cymbidium sinense* and *Cymbidium ensifolium*, recent studies indicate that regulation of peloric or pseudopeloric flower development is associated with duplication and subfunctional differentiation of the Perianth Code genes [9,12,13].

At the early developmental phase of floral organogenesis of orchid, dorsal floral organs primordia first initiate in the flower meristem, followed by ventral floral organs primordia, and, finally, column primordium initiates at the central region [9]. Therefore, there will be cis-acting elements on the Perianth Code genes that regulate the position effect in the flower primordium. Correspondingly, there will be trans-acting factors involved in the position effect regulation. TEOSINTE BRANCHED1/CYCLOIDEA/PCF (TCP) transcription factors are presumed to be associated with the determination of the dorsal–ventral position information on orchid flower primordium.

TCP transcription factors, with the conserved TCP domains, are divided into Class I (PCF or TCP-P class) and Class II (TCP-C class) [14]. Class II members are subdivided into the CIN clade and CYC/TB1 clade [15]. Previous studies only found that *CYC*-like genes control flower monosymmetry development in dicots. They contribute to establishing the dorsoventral polarity of flowers [16–26]. However, there are a few functional studies of orchid TCP transcription factors. In *Orchis italica*, 12 independent *TCP* gene fragments from the inflorescence transcriptome database are identified, but there are no members of the *CYC/TB1* clade. Using the primers designed based on the *CYC/TB1*-like gene sequence of *Phalaenopsis equestris*, *Oitatb1* is amplified from the genomic DNA of *Orchis italica*. However, the expression of *Oitatb1* cannot be detected in inflorescences [27]. In *Phalaenopsis*, three *CYC*-like genes are isolated, and functional analysis shows that *PhCYC2* and *PhCYC3* contribute to the ventral petal identity and are associated with labellum development [28]. Using the genome database of *Phalaenopsis equestris*, 23 *TCP* genes including Class I and Class II members are characterized. Functional analysis indicates that *PePCF10* and *PeCIN8* play an important role in orchid ovule development by regulating cell proliferation [29].

Erycina pusilla can be used as a model plant to study flowering physiology, pollination behavior and gene function of orchids because of its short growth cycle, flowering in bottles and small genome [30]. However, there is no report on the characterization and function of *TCP* genes in *Erycina pusilla*. Therefore, we characterized the expression patterns of *EpTCPs* isolated from the reported *Erycina pusilla* transcriptome data [30]. Then, three flower development-related genes (the *CYC/TB1* clade *EpTCP25*, the *CIN* clade *EpTCP11* and *EpTCP26*), whose expression level was relatively high in the labellum, were ectopically expressed in *Arabidopsis* to analyze their functions in plant growth and flower development. Our results provide molecular evidence that besides *CYC*-like genes, *CIN*-like genes also played roles in the control of orchid unique flower-type development.

2. Materials and Methods

2.1. Plant Materials

The *Erycina pusilla* plantlets were kept in the tissue culture room at 25 ± 2 °C under 16 h light/8 h dark photoperiod. The *Arabidopsis* (Col-0) were grown in the growth chamber (22 °C, 16 h of light per day).

2.2. TCP Family Members Identification and Phylogenetic Analysis

The TCP protein sequences of *Arabidopsis* were obtained from the NCBI database and accession numbers were listed in Supplementary Table S1. These AtTCP amino acid sequences were used to search homologous unigenes from the reported *Erycina pusilla* unigene database [30] by the tblastn in BioEdit Sequence Alignment Editor software (version 7.1.9). The candidate unigenes were translated into amino acid sequences before analysis of the conserved TCP domain using the online tool CDD from NCBI (https://www.ncbi.nlm.nih.gov/Structure/cdd/wrpsb.cgi) (accessed on 10 February 2017). The deduced amino acid sequences of *Arabidopsis* and *Erycina pusilla* TCP transcription factors were aligned using MEGA6, and the well-aligned sequences were further processed to generate Neighbor-joining trees under 1000 replicates of bootstrap iterations [31].

2.3. Relative Expression Analysis of EpTCPs

Total RNA from various tissue parts of *Erycina pusilla* was extracted from different tissues using the RNAprep Pure Plant Kit (Polysaccharides and Polyphenolics-rich) (Tiangen, Beijing, China). A 1 μg aliquot of total RNA was reverse transcribed according to the instruction manual of the PrimeScript RT reagent Kit with gDNA Eraser (TaKaRa, Dalian, China). The qPCR assays were performed using the SYBR® Green PCR Master Mix (Applied Biosystems, Waltham, MA, USA) on a Roche LightCycler 480 (Roche Applied Science, Penzberg, Upper Bavaria, Germany) according to its manual. Relative expression was calculated using the $2^{-\Delta\Delta CT}$ method with *ACTIN* as the reference gene [32]. The *ACTIN* gene sequence was obtained from the reported *Erycina pusilla* unigene database [30] according to Nr annotation. Each measurement was carried out in triplicate with three biological replicates. Graphs were constructed by GraphPad Prism 9.0 (GraphPad Software). All the primer sequences used in qPCR are shown in Supplementary Table S2.

2.4. Arabidopsis Transformation

The coding sequences of *EpTCP11* (Genbank accession number: PP515908), *EpTCP25* (Genbank accession number: PP515909) and *EpTCP26* (Genbank accession number: PP515910) were amplified, respectively, using the following primer pairs: 5′- ACGGGGGACTCTTGACC ATGGAT-ATGGAAAGTGATGAGATGTATTCG -3′ and 5′- AAGTTCTTCTCCTTTACTAGTC A-GATCTATACCCTTACCATCTCCTTTCAGTT -3′, 5′- ACGGGGGACTCTTGACCATG-GATATGTATAACCCCCCATCCCCC -3′ and 5′- AAGTTCTTCTCCTTTACTAGTCAG-ATCT ATAACCCTAACAACATTACCTTCCTC -3′, 5′- ACGGGGGACTCTTGACCATG-GATATGCC CATCTCCCACATTATTC -3′ and 5′- AAGTTCTTCTCCTTTACTAGTCA-GATCTATATGATAT GGCATGCTGTCAAGC -3′. The amplified products were cloned into the pCAMBIA1302 vector double digested at the restriction sites NcoI and BglII using a ClonExpress II One Step Cloning Kit (Vazyme, Nanjing, China). The recombinant plasmids were further transformed into the *Agrobacterium tumefaciens* EHA105 strains. The *Agrobacterium*-mediated plant transformation was performed using the floral dipping method [33]. Seeds of *35S:EpTCP11*, *35S:EpTCP25* and *35S:EpTCP26* transgenic plants were selected on half-strength Murashige and Skoog (MS) medium supplemented with 20 mg L^{-1} Hygromycin B (Roche, Shanghai, China). The hygromycin-resistant plants were identified by PCR. Three independent lines of *35S:EpTCP11*, *35S:EpTCP25* and *35S:EpTCP26* transgenic *Arabidopsis* plants were selected randomly to carry out real-time PCR detection and phenotypic analysis.

2.5. Statistical Analysis

Data were analyzed in Microsoft Excel 2016. All data were expressed as means ± SD. Statistical analysis was performed by *t*-test. $p < 0.05$ and $p < 0.01$ are considered statistically significant.

3. Results

3.1. Phylogeny of TCP Transcript Factors from Erycina pusilla

Fifteen *TCP* genes were confirmed from the reported *Erycina pusilla* unigene database [30]. A phylogenetic tree was constructed using 15 *Erycina pusilla* TCP transcript factors (EpTCPs) and 21 Arabidopsis TCP transcript factors (AtTCPs) (Figure 1). Based on the *AtTCP* gene family grouping information [14], two types of TCP can be distinguished: Class I, which is only formed by the PCF clade, and Class II, which can be further subdivided into the CYC/TB1 clade and CIN clade. The PCF clade contained EpTCP1, EpTCP10, EpTCP12, EpTCP15, EpTCP17, EpTCP20, EpTCP22 and EpTCP24. The CYC/TB1 clade contained EpTCP25, whereas the CIN clade contained EpTCP2, EpTCP5, EpTCP11, EpTCP14, EpTCP21 and EpTCP26.

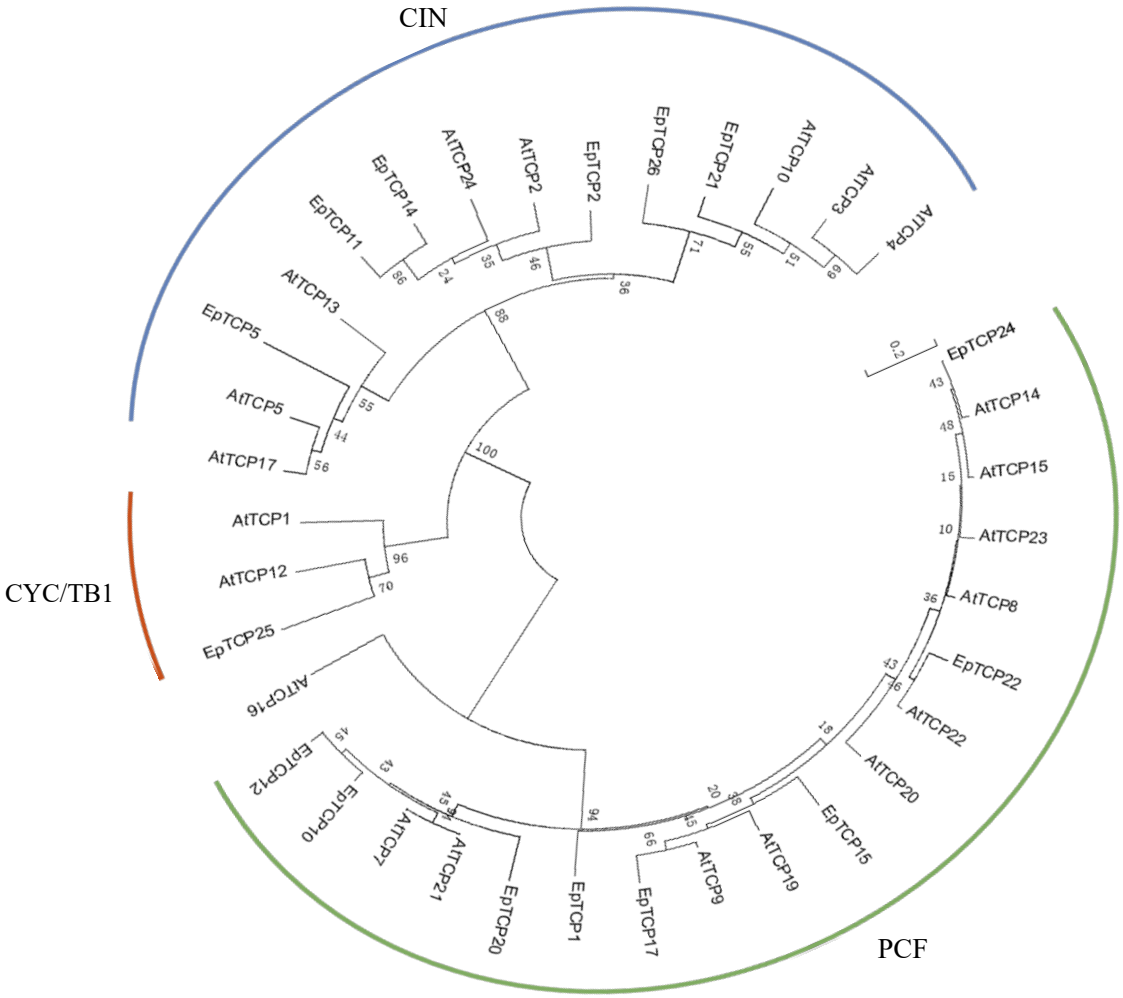

Figure 1. Phylogenetic tree of TCP transcription factors from *Erycina pusilla* and *Arabidopsis*. Different colored bands represent different subgroups. The accession numbers of sequences used for phylogeny from GenBank are as follows: AtTCP1 (NP_001077781.1); AtTCP2 (NP_001078407.1); AtTCP3 (NP_001322492.1); AtTCP4 (NP_001189896.1); AtTCP5 (NP_200905.1); AtTCP7 (NP_197719.1); AtTCP8 (NP_176107.1); AtTCP9 (NP_182092.1); AtTCP10 (NP_565712.1); AtTCP12 (NP_177047.2); AtTCP13 (NP_850501.1); AtTCP14 (NP_190346.2); AtTCP15 (NP_564973.1); AtTCP16 (NP_190101.1); AtTCP17 (NP_001318505.1); AtTCP19 (NP_200004.1); AtTCP20 (NP_001327814.1); AtTCP21 (NP_196450.1); AtTCP22 (NP_177346.1); AtTCP23 (NP_174789.1); AtTCP24 (NP_564351.1).

3.2. Expression Patterns of the EpTCP Genes in Different Tissues

Quantitative real-time PCR was performed to analyze the expression patterns of the fifteen *EpTCP* genes in various tissues of *Erycina pusilla*. The examination tissues including leaves, roots, inflorescences the length of 1~2 mm (I1), inflorescences the length of 3~4 mm (I2), floral buds the length of 3~4 mm (B1) and floral buds the length of 5~7 mm (B2) (Figure 2A). The B2 stage floral bud has completed labellum specialization. Although the morphology of the labellum has not yet been specialized, each round of floral organs in the B1 stage floral bud can be separated, whereas it is difficult to isolate floral organs from the floral bud whose developmental stage is earlier than B1.

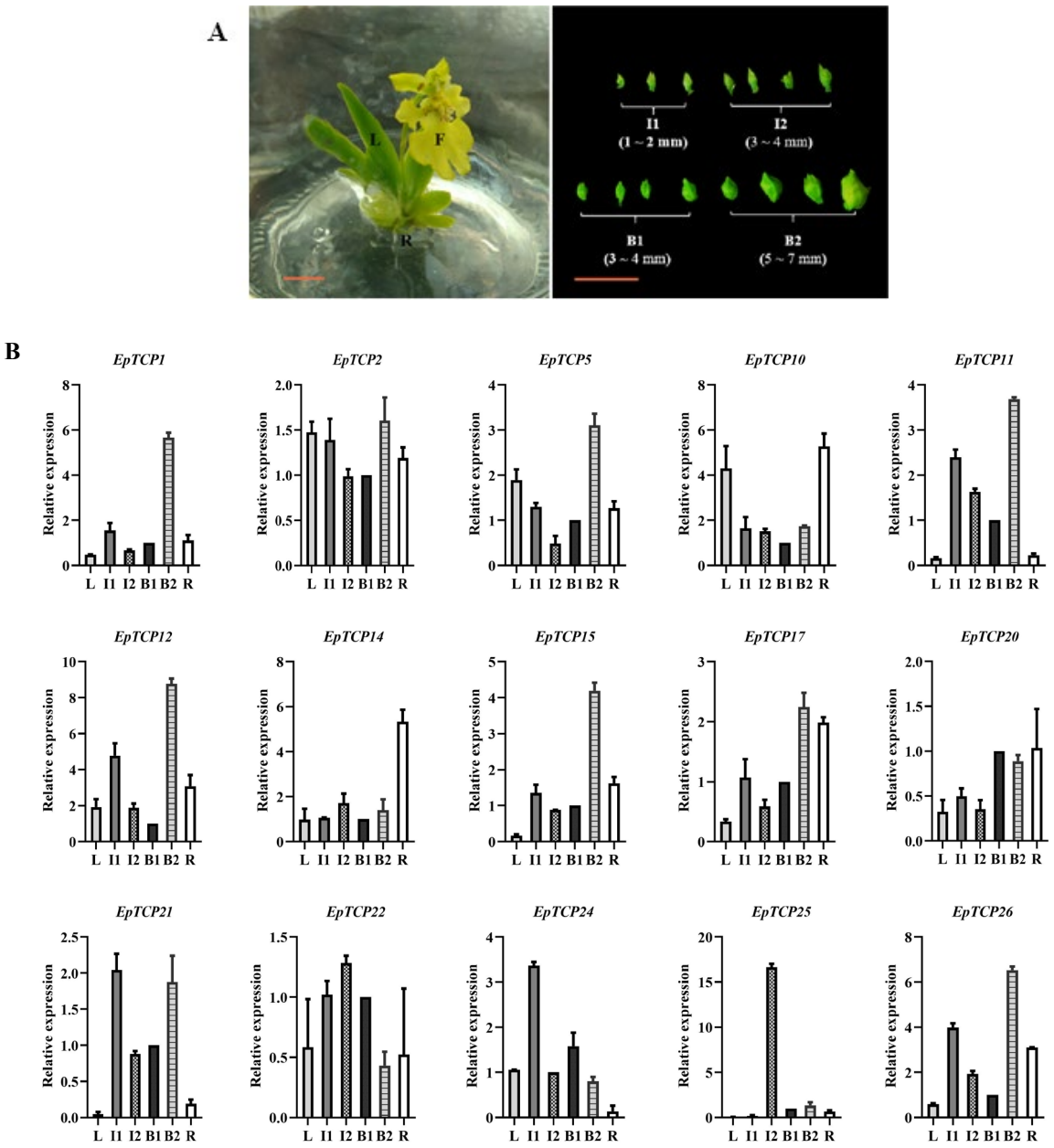

Figure 2. Relative expression of *EpTCPs* in different tissue materials of *Erycina pusilla*. (**A**) Plantlet, different periods of inflorescences and floral buds; bar = 20 mm. (**B**) qPCR assay. F, flower; L, leaf; R, root; I1, inflorescence length of 1~2 mm; I2, inflorescence length of 3~4 mm; B1, floral bud length of 3~4 mm; B2, floral bud length of 5~7 mm.

The relative expression levels of *EpTCPs* are shown in Figure 2B. *EpTCP25* showed a remarkable expression level in I2 stage inflorescences, while the expression of *EpTCP14* was highest in roots and low in other tissues. The expression levels of *EpTCP11* and *EpTCP21* were relatively high in B2-stage floral buds and I1-stage inflorescences, moderate in I2-stage inflorescences and B1-stage floral buds, and low in leaves and roots. *EpTCP12* and *EpTCP26* were mainly expressed in B2-stage floral buds and I1-stage inflorescences; however, the expression of *EpTCP12* in leaves and roots was higher than that in B1-stage floral buds and I2-stage inflorescences. *EpTCP22* showed relatively high expression in inflorescences and B1-stage floral buds, while the expression level was higher in leaves and roots than in B2-stage floral buds. The relative expression of *EpTCP24* was highest in I1-stage inflorescences and lowest in roots, whereas *EpTCP1*, *EpTCP5* and *EpTCP15* showed the highest expression

in B2-stage floral buds. *EpTCP2* and *EpTCP10* showed much higher accumulation in leaves and roots than in inflorescences and floral buds. *EpTCP17* and *EpTCP20* were highly expressed in roots, which was close to the expression level in floral buds.

3.3. Expression Patterns of the EpTCP Genes in Different Floral Organs

According to the expression patterns of *EpTCP* genes in different tissues, we selected four genes (*EpTCP11*, *EpTCP24*, *EpTCP25* and *EpTCP26*), which showed low expression in leaves and roots but high expression in inflorescences. What is more, the highest relative expression level was higher than 2. To further analyze the expression patterns in various floral organs, B1-stage floral buds were dissected into five parts (Figure 3A), including two dorsal outer tepals (OT-D), one ventral outer tepal (OT-V), one dorsal labellum (L-D), two ventral inner tepals (IT-V) and a column (C).

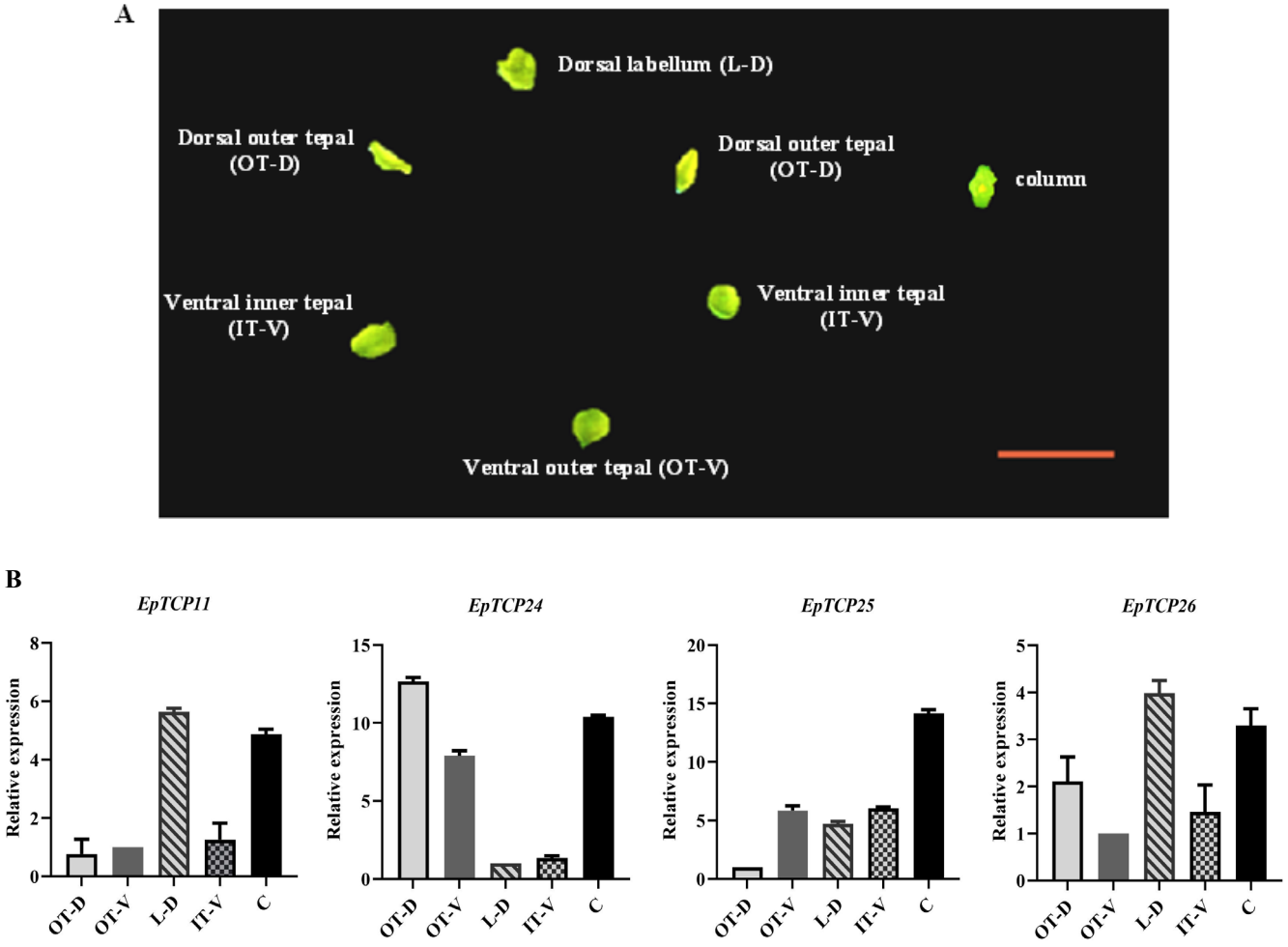

Figure 3. Relative expression of *EpTCPs* in different floral organs of *Erycina pusilla* floral bud about 4 mm. (**A**) Floral organ pattern of floral bud; bar = 20 mm. (**B**) qPCR assay. OT-D, dorsal outer tepal; OT-V, ventral outer tepal; L-D, dorsal labellum; IT-V, ventral inner tepal; C, column.

The qPCR assay of the four *EpTCP* genes is shown in Figure 3B. The results showed that the four *EpTCP* genes were highly expressed in the column tissues. And the expression pattern of these four *EpTCPs* in different tepals was as follows: *EpTCP24* is mainly expressed in outer tepals, while the expression of *EpTCP25* was relatively high in ventral outer tepal, dorsal labellum and ventral inner tepals when compared with dorsal outer tepals. *EpTCP11* and *EpTCP26* showed the highest expression level in the dorsal labellum. Furthermore, *EpTCP26* showed higher expression in dorsal outer tepals than in ventral outer tepals. All

the results indicated that *EpTCP26* showed differential expression along the dorsoventral polarity of tepals, which was high in the dorsal and low in the ventral.

3.4. Phenotypes of EpTCP11, EpTCP25 or EpTCP26 Overexpression in Arabidopsis

Based on the results of expression patterns in different floral organs, we selected *EpTCP11*, *EpTCP25* and *EpTCP26*, whose expression levels were relatively high in the labellum, to verify the function by ectopically expressing them in *Arabidopsis*, respectively. The presence of the transgene in transgenic lines was confirmed by PCR (Supplementary Figure S1). Three independent lines of *35S:EpTCP11*, *35S:EpTCP25* and *35S:EpTCP26* transgenic *Arabidopsis* plants were selected randomly to carry out a phenotypic analysis. The results of real-time PCR showed that exogenous *EpTCP* was expressed in all the selected transgenic lines (Supplementary Figure S2).

3.4.1. Effects of *EpTCP11*, *EpTCP25* or *EpTCP26* Overexpression on the Primary Root Growth of *Arabidopsis*

The seeds of *35S:EpTCP11*, *35S:EpTCP25* and *35S:EpTCP26* transgenic *Arabidopsis* were germinated on MS medium for 7 days, and then the primary root lengths were measured. As shown in Figure 4, overexpression of *EpTCP11* or *EpTCP25* significantly inhibited the elongation of *Arabidopsis* primary roots. *EpTCP11* overexpression inhibited primary root growth most severely, and the root lengths shortened by 40%~50%. In contrast, overexpression of *EpTCP26* significantly promoted the elongation of primary roots in *Arabidopsis*.

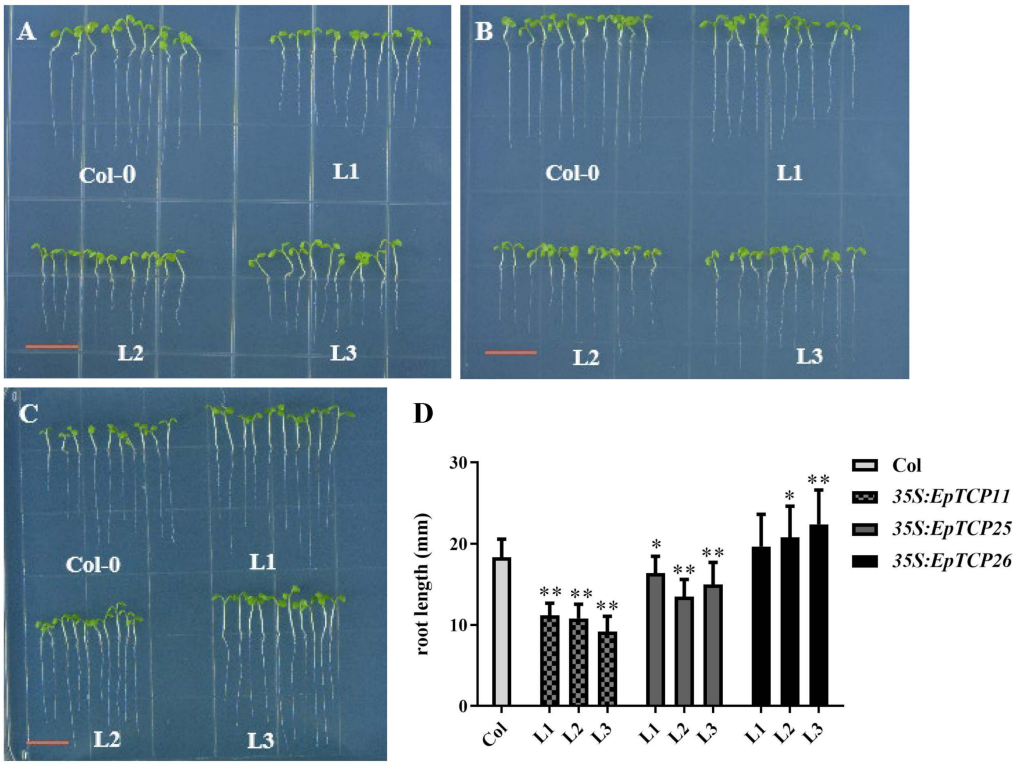

Figure 4. Root growth of 7-day-old Col-0, three independent lines of *35S:EpTCP11* (**A**), *35S:EpTCP25* (**B**) and *35S:EpTCP26* (**C**) transgenic *Arabidopsis*; bar = 10 mm. (**D**) Root lengths of Col-0 and transgenic *Arabidopsis* plants. Asterisks indicated significant differences between transgenic *Arabidopsis* and Col-0 (* $p < 0.05$, ** $p < 0.01$).

3.4.2. Effects of *EpTCP11*, *EpTCP25* or *EpTCP26* Overexpression on the Plant Growth and Development of *Arabidopsis*

The wild-type and transgenic *Arabidopsis* plants were transplanted into nutrient soil after growing on MS medium for 7 days. About 15 days after transplantation, the wild-

type and transgenic *Arabidopsis* plants began to bolt in succession. The leaf size and rosette leaf number of *35S:EpTCP11* transgenic plants (Figure 5B–D,K) were almost the same as the Col wild-type *Arabidopsis* (Figure 5A,K), while in *35S:EpTCP26* transgenic plants, leaves were larger than those of the Col wild-type *Arabidopsis* (Figure 5H–J), but the number of rosette leaves was not significantly different from that of the wild-type *Arabidopsis* (Figure 5K). Compared with the Col wild-type *Arabidopsis*, the rosette leaf number of *35S:EpTCP25* transgenic plants was significantly increased, which indicates that overexpression of *EpTCP25* delayed the flowering time (Figure 5E–G,K).

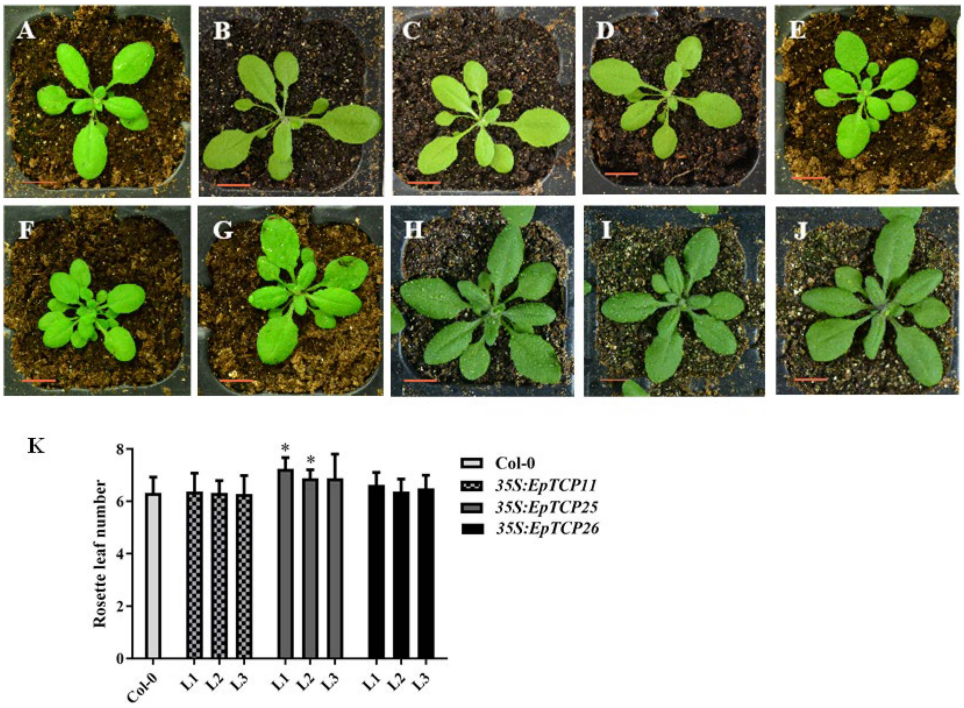

Figure 5. Growth of Col-0 (**A**), three independent lines of *35S:EpTCP11* (**B**–**D**), *35S:EpTCP25* (**E**–**G**) and *35S:EpTCP26* (**H**–**J**) transgenic *Arabidopsis* plants after 15 days of transplant; bar = 10 mm. (**K**) Statistical rosette leaf numbers of Col-0 and transgenic *Arabidopsis* when flowering. Asterisks indicated significant different between transgenic *Arabidopsis* and Col-0 (* $p < 0.05$).

3.4.3. Effects of *EpTCP11*, *EpTCP25* or *EpTCP26* Overexpression on the Floral Organs Development of *Arabidopsis*

The flowers of *35S:EpTCP11*, *35S:EpTCP25* and *35S:EpTCP26* transgenic *Arabidopsis* were observed for a week from the beginning of flowering. There were four phenotypic variations of flowers in the transgenic *Arabidopsis*. Flowers with phenotypic variation 1 changed from radial symmetry to bilateral symmetry with one petal shortened (Figure 6B), while flowers with phenotypic variation 2 changed from radial symmetry to bilateral symmetry with two adjacent petals shortened (Figure 6C). Flowers with phenotypic variation 3 exhibited a petaloid structure at the top of one stamen (Figure 6F). And flowers with phenotypic variation 4 showed stamenoid structure at the petal margin (Figure 6G).

Flowers of *35S:EpTCP11* transgenic *Arabidopsis* had the highest probability of phenotypic variation 1 and phenotypic variation 2. The variation rates of these two phenotypes reached 26–42%, which was much higher than the variation rate of wild-type *Arabidopsis* at less than 10%. Moreover, the average length of long petals and short petals of the flowers with phenotypic variation 1 and 2 in *35S:EpTCP11* transgenic *Arabidopsis* were compared with the average length of the petals of wild-type flowers, respectively. The results showed that the length of short petals was significantly different from that of wild-type flower petals, while the length of long petals was almost the same as that of wild-type flower petals (Figure 6D). All these suggested that *EpTCP11* may change the flower symmetry.

Phenotypic variations of petaloid stamen and stamenoid petal occurred in the flowers of *35S:EpTCP11*, *35S:EpTCP25* and *35S:EpTCP26* transgenic *Arabidopsis*. Although the variation rate was only 2–8%, flowers with these two phenotypic variations were not found in wild-type *Arabidopsis*. The result suggested that *EpTCP11*, *EpTCP25* and *EpTCP26* may cause the homeotic conversion of floral organs.

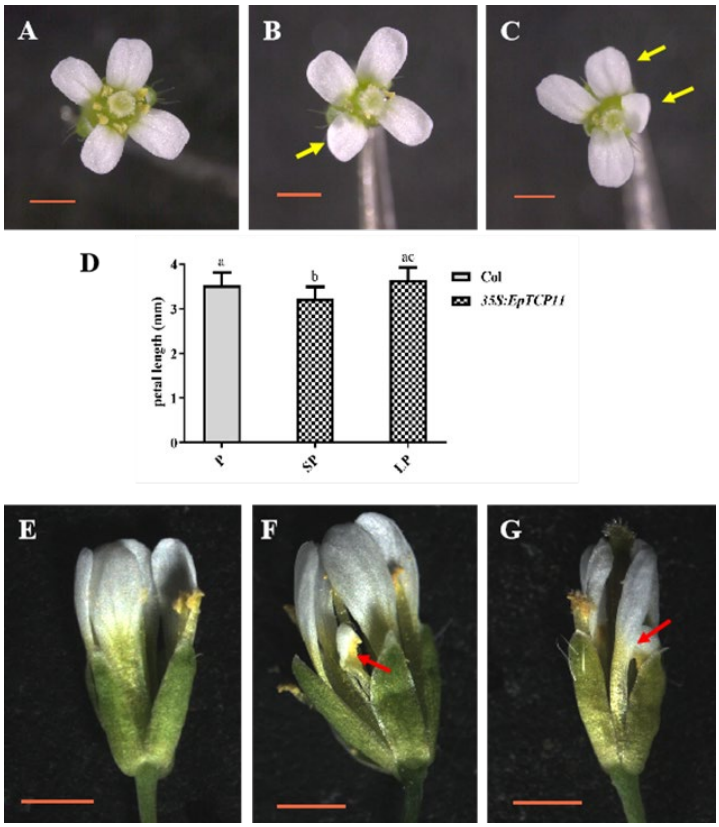

Figure 6. Flower mutations of *35S:EpTCP11*, *35S:EpTCP25* and *35S:EpTCP26* transgenic *Arabidopsis* plants. (**A**) Wild-type flower. (**B**) Flower with phenotypic variation 1; yellow arrow markers short petal. (**C**) Flower with phenotypic variation 2. (**D**) The short and long petal lengths of flowers with phenotypic variation 1 and 2 in *35S:EpTCP11* transgenic *Arabidopsis* plants; P, petals of Col-0; SP, short petals; LP, long petals. Different letters indicated significant differences in petal length ($p < 0.05$). (**E**) Side view of wild-type flower. (**F**) Side view of flower with phenotypic variation 3; red arrow markers the mutant stamen. (**G**) Side view of flower with phenotypic variation 4; red arrow markers the mutant petal. Bar = 1 mm.

4. Discussion

The coevolution of orchid flowers and pollinators leads to the highly specialized morphology of the orchid flower, which makes the orchid plant one of the ideal materials for studying flower-type development of monocotyledons. Orchid has a typical zygomorphic flower. And *CYC*-like *TCP* gene is the determinant of flower symmetry development in dicotyledons. In the present study, based on the reported *Erycina pusilla* transcriptome data [30], by expression pattern characterization and ectopically overexpression in *Arabidopsis*, we found that *CIN*-like *TCP* genes would be involved in flower symmetry development of *Erycina pusilla*.

Erycina pusilla, an orchid model species, has typically bilaterally symmetrical flowers. But identification and functional studies of TCP transcription factors have not been reported.

It has been reported that TCP transcription factors play roles in flower development from the early stage [17]. Therefore, by detecting the relative expression of *EpTCPs* in different tissues of *Erycina pusilla*, we screened out four genes that were lowly expressed in leaves and roots but highly expressed in inflorescences. Then, the expression of these four

genes was further analyzed in various flower organs using small floral buds at the B1 stage, whose labellum has not yet been specialized.

The flowers of *Erycina pusilla* are typically bilaterally symmetrical, and each whorl of tepal establishes dorsoventral asymmetry. The outer perianths can be classified into two dorsal narrow sepals and one ventral petaloid sepal, whereas the inner perianths can be classified into one dorsal well-differentiated labellum and two ventral normal petals. The qPCR assay showed that *EpTCP11* was highly expressed in the dorsal labellum, *EpTCP26* was highly expressed in the dorsal tepals including the dorsal labellum and the dorsal outer sepals, whereas *EpTCP25* was lowly expressed in the dorsal outer sepals. Therefore, we inferred that *EpTCP11*, *EpTCP25* and *EpTCP26* could be correlated with the regulation of zygomorphic flower development in *Erycina pusilla*. Phylogenetic tree analysis showed that EpTCP25 belongs to the CYC/TB1 clade while EpTCP11 and EpTCP26 belong to the CIN clade.

It is reported that members of the CYC/TB1 clade inhibit plant growth and proliferation [16,34]. Overexpression of Antirrhinum *CYC* in *Arabidopsis* represses the growth of plants and leaves [35]. Similarly, overexpression of the *CYC*-like gene *EpTCP25* in *Arabidopsis* inhibited primary root elongation and delayed flowering. However, accumulated evidence demonstrates that *CYC*-like genes play key roles in the zygomorphic flower development of dicotyledons [16–26]. In monocotyledons Commelinaceae and Zingiberales, *CYC*-like genes are predominantly expressed in the ventral petals [36,37]. In contrast, *CYC*-like genes are recruited to specialize in the development of dorsal petals in dicotyledons [38]. In *Phalaenopsis*, *PhCYC1*, *PhCYC2* and *PhCYC3* with high homology are isolated. *PhCYC2* and *PhCYC3* are highly expressed in the inner tepals (two petals and one labellum) of wild-type *Phalaenopsis equestris*, while they are lowly expressed in the labelloid petals and labellum of peloric flower (three labellums mutants). With the heterologous overexpression of *PhCYC2* and *PhCYC3* in *Torenia furnieri*, the results indicate that *PhCYC2* and *PhCYC3* contribute to the ventral petal identity and are associated with labellum development [28]. In this study, overexpression of *EpTCP25* in Arabidopsis did not change floral symmetry. This finding may be related to the fact that there was no difference in the expression of *EpTCP25* between the dorsal labellum and ventral petals. And it was possible that other TCP transcription factors were involved in the bilaterally symmetric flower development of *Erycina pusilla*.

Overexpression of the *CIN*-like gene *EpTCP11* repressed the primary root growth of *Arabidopsis* and changed the radially symmetric flower to a bilaterally symmetric flower by inhibiting the elongation of one or two adjacent petals. In contrast, overexpression of the *CIN*-like gene *EpTCP26* in *Arabidopsis* promoted primary root growth and leaf growth but did not affect petal growth. In previous studies on *Phalaenopsis equestris*, it was found that overexpression of *PeCIN8* represses plant growth of *Arabidopsis* [29]. All these indicated that different members in the same clade of *TCP* gene family have functional divergence, and even play opposite roles in the same developmental process.

Phylogenetic tree analysis showed that EpTCP11 possessed high homology with AtTCP24 and AtTCP2 of Arabidopsis. It has been reported that *AtTCP24* associates with *ABAP1* and negatively regulates the transcription of *AtCDT1a* and *AtCDT1b*, which may limit DNA replication and consequently block cell cycle progression at G1 to S [39]. *AtTCP2* can upregulate *NGA3* gene expression by activating its promoter. *NAG3* overexpression represses plant growth and makes leaves narrow and short. So, part of the *CIN*-like *TCP* role in leaf development may be mediated by *NGA3* upregulation [40]. Further experiments are needed to explore whether the molecular mechanism of *EpTCP11* in regulating primary roots and individual petals growth of *Arabidopsis* is similar to that of *AtTCP24* and *AtTCP2*.

EpTCP26 possessed high homology with AtTCP10, AtTCP3 and AtTCP4 of Arabidopsis. In *Arabidopsis*, the normal expression of the *CIN*-like *TCP* gene is critical for leaf morphogenesis [41–45]. Expression of a chimeric repressor from AtTCP3 (AtTCP3SRDX) resulted in the inhibition of main root elongation and the formation of larger leaves with wavey surfaces and serrated margins because of excessive growth in the marginal re-

gion. *AtTCP10* and *AtTCP4* have functions similar to that of *AtTCP3* [46]. In *Cyclamen persicum*, CpTCP1, which is clustered in the same group as AtTCP3 and AtTCP4, has a function similar to that of AtTCP3. Expression of CpTCP1SRDX generates larger leaves and smaller flowers with undulating edges [47]. These *CIN*-like *TCP* genes may regulate the morphogenesis of vegetative organs and flowers by suppressing boundary-specific gene expression. In this study, we observed that overexpression of *EpTCP26* in *Arabidopsis* promoted root elongation and leaf growth, but did not affect petal size. We inferred that different downstream genes could be involved in the regulatory pathway of *EpTCP26*.

Unexpectedly, overexpression of *EpTCP11*, *EpTCP25* or *EpTCP26* generated a homeotic transition of floral organs. Whether they affect the floral organ identity by regulating B and C function MADS-box genes remained to be further studied.

5. Conclusions

In this study, we screened three flower development-related *TCP* genes (the *CYC/TB1* clade *EpTCP25*, the *CIN* clade *EpTCP11* and *EpTCP26*) from the reported *Erycina pusilla* transcriptome database [30]. They all expressed relatively high levels in the dorsal labellum. Ectopic expression of these genes in Arabidopsis led to the homeotic transition of floral organs. What is more, *CIN*-like gene *EpTCP11* overexpression changed the radially symmetric flower to a bilaterally symmetric flower. Our study offered new insight for further exploring the genetic regulation of orchid floral zygomorphy.

In previous research, 'Orchid Code' and 'Perianth Code' indicate that the Perianth Code MADS-box gene duplications followed by sub-functionalization events contribute to the evolutionary origin of morphological novelties in orchids [8,9,13]. Together with our studies, we assumed that different *TCP* genes, including *CYC*-like and *CIN*-like genes, were probably recruited to interact with various MADS-box genes for distinguishing different types of floral organs during orchid evolution.

Supplementary Materials: The following supporting information can be downloaded at: https://www.mdpi.com/article/10.3390/horticulturae10060534/s1, Table S1: protein accession numbers used in this study; Table S2: primers used in qPCR; Figure S1: PCR detection of *EpTCP11* (A), *EpTCP25* (B) and *EpTCP26* (C) transgenic *Arabidopsis* plants. M, DL2000 marker; 1, blank control; 2, Col-0; 3, positive control (plasmid); 4~15, hygromycin-resistant *Arabidopsis* plants; Figure S2: Real-time PCR analysis of exogenous *EpTCP* in different tissue materials of Col-0, three independent lines of *35S:EpTCP11* (A), *35S:EpTCP25* (B) and *35S:EpTCP26* (C) transgenic *Arabidopsis* plants. L, Leaf; R, Root; I, Inflorescence; Sl, Silique.

Author Contributions: X.H. designed the research and wrote the paper; Y.-H.T. and Y.-Y.Z. performed the studies and analyzed the data. All authors have read and agreed to the published version of the manuscript.

Funding: This research was funded by the Guangdong Basic and Applied Basic Research Foundation (No. 2021A1515011086) and the Guangdong Natural Science Foundation (No. 2018A030313294).

Data Availability Statement: Data are contained in the article and Supplementary Materials.

Conflicts of Interest: The authors declare no conflicts of interest.

References

1. Aceto, S.; Gaudio, L. The MADS and the beauty: Genes involved in the development of orchid Flowers. *Curr. Genom.* **2011**, *12*, 342–356. [CrossRef] [PubMed]
2. Yu, H.; Goh, C.J. Identification and characterization of three orchid MADS-box genes of the AP1/AGL9 subfamily during floral transition. *Plant Physiol.* **2000**, *123*, 1325–1336. [CrossRef]
3. Hsu, H.F.; Huang, C.H.; Chou, L.T.; Yang, C.H. Ectopic expression of an orchid (*Oncidium* Gower Ramsey) *AGL6*-like gene promotes flowering by activating flowering time genes in *Arabidopsis thaliana*. *Plant Cell Physiol.* **2003**, *44*, 783–794. [CrossRef] [PubMed]
4. Tsai, W.C.; Kuoh, C.S.; Chuang, M.H.; Chen, W.H.; Chen, H.H. Four *DEF*-like MADS box genes displayed distinct floral morphogenetic roles in *Phalaenopsis* orchid. *Plant Cell Physiol.* **2004**, *45*, 831–844. [CrossRef] [PubMed]

5. Xu, Y.; Teo, L.L.; Zhou, J.; Kumar, P.P.; Yu, H. Floral organ identity genes in the orchid *Dendrobium crumenatum*. *Plant J.* **2006**, *46*, 54–68. [CrossRef]
6. Tsai, W.C.; Pan, Z.J.; Hsiao, Y.Y.; Jeng, M.F.; Wu, T.F.; Chen, W.H.; Chen, H.H. Interactions of B-class complex proteins involved in tepal development in *Phalaenopsis* orchid. *Plant Cell Physiol.* **2008**, *49*, 814–824. [CrossRef] [PubMed]
7. Chang, Y.Y.; Chiu, Y.F.; Wu, J.W.; Yang, C.H. Four orchid (*Oncidium* Gower Ramsey) *AP1/AGL9*-like MADS box genes show novel expression patterns and cause different effects on floral transition and formation in *Arabidopsis thaliana*. *Plant Cell Physiol.* **2009**, *50*, 1425–1438. [CrossRef] [PubMed]
8. Mondragón-Palomino, M.; Theissen, G. Conserved differential expression of paralogous *DEFICIENS*- and *GLOBOSA*-like MADS-box genes in the flowers of Orchidaceae: Refining the 'orchid code'. *Plant J.* **2011**, *66*, 1008–1019. [CrossRef] [PubMed]
9. Su, S.; Shao, X.; Zhu, C.; Xu, J.; Lu, H.; Tang, Y.; Jiao, K.; Guo, W.; Xiao, W.; Liu, Z.; et al. Transcriptome-Wide Analysis Reveals the Origin of Peloria in Chinese Cymbidium (*Cymbidium sinense*). *Plant Cell Physiol.* **2018**, *59*, 2064–2074. [CrossRef]
10. Mondragón-Palomino, M.; Theissen, G. Why are orchid flowers so diverse? Reduction of evolutionary constraints by paralogues of class B floral homeotic genes. *Ann. Bot.* **2009**, *104*, 583–594. [CrossRef]
11. Hsu, H.F.; Hsu, W.H.; Lee, Y.I.; Mao, W.T.; Yang, J.Y.; Li, J.Y.; Yang, C.H. Model for perianth formation in orchids. *Nat. Plants* **2015**, *1*, 15046. [CrossRef]
12. Wei, Y.; Jin, J.; Yao, X.; Lu, C.; Zhu, G.; Yang, F. Transcriptome analysis reveals clues into leaf-like flower mutant in Chinese orchid *Cymbidium ensifolium*. *Plant Divers.* **2020**, *42*, 92–101. [CrossRef] [PubMed]
13. Yang, F.X.; Gao, J.; Wei, Y.L.; Ren, R.; Zhang, G.Q.; Lu, C.Q.; Jin, J.P.; Ai, Y.; Wang, Y.Q.; Chen, L.J.; et al. The genome of *Cymbidium sinense* revealed the evolution of orchid traits. *Plant Biotechnol. J.* **2021**, *19*, 2501–2516. [CrossRef] [PubMed]
14. Martín-Trillo, M.; Cubas, P. TCP genes: A family snapshot ten years later. *Trends Plant Sci.* **2010**, *15*, 31–39. [CrossRef] [PubMed]
15. Horn, S.; Pabón-Mora, N.; Theuß, V.S.; Busch, A.; Zachgo, S. Analysis of the CYC/TB1 class of TCP transcription factors in basal angiosperms and magnoliids. *Plant J.* **2015**, *81*, 559–571. [CrossRef] [PubMed]
16. Luo, D.; Carpenter, R.; Vincent, C.; Copsey, L.; Coen, E. Origin of floral asymmetry in *Antirrhinum*. *Nature* **1996**, *383*, 794–799. [CrossRef] [PubMed]
17. Luo, D.; Carpenter, R.; Copsey, L.; Vincent, C.; Clark, J.; Coen, E. Control of organ asymmetry in flowers of *Antirrhinum*. *Cell* **1999**, *99*, 367–376. [CrossRef] [PubMed]
18. Feng, X.; Zhao, Z.; Tian, Z.; Xu, S.; Luo, Y.; Cai, Z.; Wang, Y.; Yang, J.; Wang, Z.; Weng, L.; et al. Control of petal shape and floral zygomorphy in *Lotus japonicus*. *Proc. Natl. Acad. Sci. USA* **2006**, *103*, 4970–4975. [CrossRef] [PubMed]
19. Busch, A.; Zachgo, S. Control of corolla monosymmetry in the Brassicaceae *Iberis amara*. *Proc. Natl. Acad. Sci. USA* **2007**, *104*, 16714–16719. [CrossRef]
20. Zhang, W.; Kramer, E.M.; Davis, C.C. Floral symmetry genes and the origin and maintenance of zygomorphy in a plant-pollinator mutualism. *Proc. Natl. Acad. Sci. USA* **2010**, *107*, 6388–6393. [CrossRef]
21. Yang, X.; Pang, H.B.; Liu, B.L.; Qiu, Z.J.; Gao, Q.; Wei, L.; Dong, Y.; Wang, Y.Z. Evolution of double positive autoregulatory feedback loops in CYCLOIDEA2 clade genes is associated with the origin of floral zygomorphy. *Plant Cell* **2012**, *24*, 1834–1847. [CrossRef] [PubMed]
22. Xu, S.; Luo, Y.; Cai, Z.; Cao, X.; Hu, X.; Yang, J.; Luo, D. Functional diversity of *CYCLOIDEA*-like TCP genes in the control of zygomorphic flower development in *Lotus japonicus*. *J. Integr. Plant Biol.* **2013**, *55*, 221–231. [CrossRef] [PubMed]
23. Dong, Y.; Liu, J.; Li, P.W.; Li, C.Q.; Lü, T.F.; Yang, X.; Wang, Y.Z. Evolution of Darwin's *Peloric* Gloxinia (*Sinningia speciosa*) is caused by a null mutation in a pleiotropic TCP Gene. *Mol. Biol. Evol.* **2018**, *35*, 1901–1915. [CrossRef] [PubMed]
24. Li, X.; Sun, M.; Jia, Y.; Qiu, D.; Peng, Q.; Zhuang, L. Genetic control of the lateral petal shape and identity of asymmetric flowers in mungbean (*Vigna radiata* L.). *Front. Plant Sci.* **2022**, *13*, 996239. [CrossRef] [PubMed]
25. Tong, J.; Knox, E.B.; Morden, C.W.; Cellinese, N.; Mossolem, F.; Zubair, A.S.; Howarth, D.G. Duplication and expression patterns of *CYCLOIDEA*-like genes in Campanulaceae. *EvoDevo* **2022**, *13*, 5. [CrossRef] [PubMed]
26. Zhao, H.; Liao, H.; Li, S.; Zhang, R.; Dai, J.; Ma, P.; Wang, T.; Wang, M.; Yuan, Y.; Fu, X.; et al. Delphinieae flowers originated from the rewiring of interactions between duplicated and diversified floral organ identity and symmetry genes. *Plant Cell* **2023**, *35*, 994–1012. [CrossRef] [PubMed]
27. De Paolo, S.; Gaudio, L.; Aceto, S. Analysis of the *TCP* genes expressed in the inflorescence of the orchid *Orchis italica*. *Sci. Rep.* **2015**, *5*, 16265. [CrossRef]
28. Liao, X.Z. Bioinformatic Analysis of TCP Genes in Orchidaceae and Cloning and Functional Study of *CYC*-like Genes in *Phalaenopsis*. Master's Thesis, Nanjing Agricultural University, Nanjing, China, 2017.
29. Lin, Y.F.; Chen, Y.Y.; Hsiao, Y.Y.; Shen, C.Y.; Hsu, J.L.; Yeh, C.M.; Mitsuda, N.; Ohme-Takagi, M.; Liu, Z.J.; Tsai, W.C. Genome-wide identification and characterization of *TCP* genes involved in ovule development of *Phalaenopsis equestris*. *J. Exp. Bot.* **2016**, *67*, 5051–5066. [CrossRef]
30. Chou, M.L.; Shih, M.C.; Chan, M.T.; Liao, S.Y.; Hsu, C.T.; Haung, Y.T.; Chen, J.J.; Liao, D.C.; Wu, F.H.; Lin, C.S. Global transcriptome analysis and identification of a CONSTANS-like gene family in the orchid Erycina pusilla. *Planta* **2013**, *237*, 1425–1441. [CrossRef]
31. Tamura, K.; Stecher, G.; Peterson, D.; Filipski, A.; Kumar, S. MEGA6: Molecular evolutionary genetics analysis version 6.0. *Mol. Biol. Evol.* **2013**, *30*, 2725–2729. [CrossRef]

32. Zhu, G.; Yang, F.; Shi, S.; Li, D.; Wang, Z.; Liu, H.; Huang, D.; Wang, C. Transcriptome characterization of *Cymbidium sinense* 'dharma' using 454 pyrosequencing and its application in the identification of genes associated with leaf color variation. *PLoS ONE* **2015**, *10*, e128592. [CrossRef]
33. Clough, S.J.; Bent, A.F. Floral dip: A simplified method for *Agrobacterium*-mediated transformation of *Arabidopsis thaliana*. *Plant J.* **1998**, *16*, 735–743. [CrossRef] [PubMed]
34. Aguilar-Martínez, J.A.; Poza-Carrión, C.; Cubas, P. *Arabidopsis BRANCHED1* acts as an integrator of branching signals within axillary buds. *Plant Cell* **2007**, *19*, 458–472. [CrossRef] [PubMed]
35. Costa, M.M.; Fox, S.; Hanna, A.I.; Baxter, C.; Coen, E. Evolution of regulatory interactions controlling floral asymmetry. *Development* **2005**, *132*, 5093–5101. [CrossRef] [PubMed]
36. Bartlett, M.E.; Specht, C.D. Changes in expression pattern of the *teosinte branched1*-like genes in the Zingiberales provide a mechanism for evolutionary shifts in symmetry across the order. *Am. J. Bot.* **2011**, *98*, 227–243. [CrossRef] [PubMed]
37. Preston, J.C.; Hileman, L.C. Parallel evolution of TCP and B-class genes in Commelinaceae flower bilateral symmetry. *EvoDevo* **2012**, *3*, 6. [CrossRef] [PubMed]
38. Hileman, L.C. Trends in flower symmetry evolution revealed through phylogenetic and developmental genetic advances. *Philos. Trans. R. Soc. Lond B Biol. Sci.* **2014**, *369*, 20130348. [CrossRef] [PubMed]
39. Masuda, H.P.; Cabral, L.M.; De Veylder, L.; Tanurdzic, M.; de Almeida Engler, J.; Geelen, D.; Inzé, D.; Martienssen, R.A.; Ferreira, P.C.; Hemerly, A.S. ABAP1 is a novel plant Armadillo BTB protein involved in DNA replication and transcription. *EMBO J.* **2008**, *27*, 2746–2756. [CrossRef] [PubMed]
40. Ballester, P.; Navarrete-Gómez, M.; Carbonero, P.; Oñate-Sánchez, L.; Ferrándiz, C. Leaf expansion in *Arabidopsis* is controlled by a TCP-NGA regulatory module likely conserved in distantly related species. *Physiol. Plant* **2015**, *155*, 21–32. [CrossRef]
41. Palatnik, J.F.; Allen, E.; Wu, X.; Schommer, C.; Schwab, R.; Carrington, J.C.; Weigel, D. Control of leaf morphogenesis by microRNAs. *Nature* **2003**, *425*, 257–263. [CrossRef]
42. Schommer, C.; Palatnik, J.F.; Aggarwal, P.; Chételat, A.; Cubas, P.; Farmer, E.E.; Nath, U.; Weigel, D. Control of jasmonate biosynthesis and senescence by miR319 targets. *PLoS Biol.* **2008**, *6*, e230. [CrossRef] [PubMed]
43. Koyama, T.; Mitsuda, N.; Seki, M.; Shinozaki, K.; Ohme-Takagi, M. TCP transcription factors regulate the activities of ASYMMETRIC LEAVES1 and miR164, as well as the auxin response, during differentiation of leaves in *Arabidopsis*. *Plant Cell* **2010**, *22*, 3574–3588. [CrossRef] [PubMed]
44. Koyama, T.; Sato, F.; Ohme-Takagi, M. Roles of miR319 and TCP transcription factors in leaf development. *Plant Physiol.* **2017**, *175*, 874–885. [CrossRef] [PubMed]
45. Lan, J.; Qin, G. The Regulation of CIN-like TCP Transcription Factors. *Int. J. Mol. Sci.* **2020**, *21*, 4498. [CrossRef] [PubMed]
46. Koyama, T.; Furutani, M.; Tasaka, M.; Ohme-Takagi, M. TCP transcription factors control the morphology of shoot lateral organs via negative regulation of the expression of boundary-specific genes in *Arabidopsis*. *Plant Cell* **2007**, *19*, 473–484. [CrossRef]
47. Tanaka, Y.; Yamamura, T.; Oshima, Y.; Mitsuda, N.; Koyama, T.; Ohme-Takagi, M.; Terakawa, T. Creating ruffled flower petals in Cyclamen persicum by expression of the chimeric cyclamen TCP repressor. *Plant Biotechnol.* **2011**, *28*, 141–147. [CrossRef]

Disclaimer/Publisher's Note: The statements, opinions and data contained in all publications are solely those of the individual author(s) and contributor(s) and not of MDPI and/or the editor(s). MDPI and/or the editor(s) disclaim responsibility for any injury to people or property resulting from any ideas, methods, instructions or products referred to in the content.